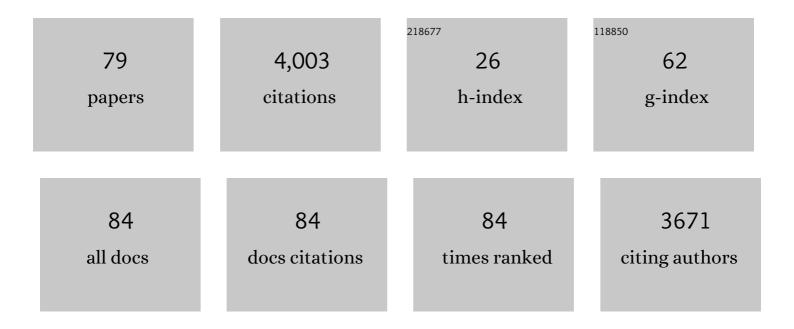
List of Publications by Year in descending order

Source: https://exaly.com/author-pdf/4793165/publications.pdf Version: 2024-02-01



#	Article	lF	CITATIONS
1	Deformation Twinning in Nanocrystalline Aluminum. Science, 2003, 300, 1275-1277.	12.6	1,058
2	Shock-Induced Localized Amorphization in Boron Carbide. Science, 2003, 299, 1563-1566.	12.6	483
3	In situ TEM observations of fast grain-boundary motion in stressed nanocrystalline aluminum films. Acta Materialia, 2008, 56, 3380-3393.	7.9	372
4	Microstructural evolution of pure magnesium under high strain rate loading. Acta Materialia, 2015, 87, 56-67.	7.9	168
5	Characterizing deformed ultrafine-grained and nanocrystalline materials using transmission Kikuchi diffraction in a scanning electron microscope. Acta Materialia, 2014, 62, 69-80.	7.9	142
6	Modelling the flow stress anomaly in Î ³ -TiAl I. Experimental observations of dislocation mechanisms. Philosophical Magazine A: Physics of Condensed Matter, Structure, Defects and Mechanical Properties, 1995, 71, 1295-1312.	0.6	136
7	Mechanistic Insights for Low-Overpotential Electroreduction of CO ₂ to CO on Copper Nanowires. ACS Catalysis, 2017, 7, 8578-8587.	11.2	106
8	Pyramidal I slip in c-axis compressed Mg single crystals. Scripta Materialia, 2016, 112, 75-78.	5.2	105
9	Microstructural characterization of boron-rich boron carbide. Acta Materialia, 2017, 136, 202-214.	7.9	91
10	Size Effects in the Mechanical Properties of Bulk Bicontinuous Ta/Cu Nanocomposites Made by Liquid Metal Dealloying. Advanced Engineering Materials, 2016, 18, 46-50.	3.5	75
11	Nanotwinned metal MEMS films with unprecedented strength and stability. Science Advances, 2017, 3, e1700685.	10.3	68
12	Superstrength through Nanotwinning. Nano Letters, 2016, 16, 7573-7579.	9.1	62
13	Atomic-Level Understanding of "Asymmetric Twins―in Boron Carbide. Physical Review Letters, 2015, 115, 175501.	7.8	56
14	MATERIALS SCIENCE: Understanding How Nanocrystalline Metals Deform. Science, 2004, 304, 221-223.	12.6	50
15	New Ground-State Crystal Structure of Elemental Boron. Physical Review Letters, 2016, 117, 085501.	7.8	44
16	Nucleation of amorphous shear bands at nanotwins in boron suboxide. Nature Communications, 2016, 7, 11001.	12.8	43
17	Experimental observations of amorphization in stoichiometric and boron-rich boron carbide. Acta Materialia, 2019, 181, 207-215.	7.9	43
18	Locating Si atoms in Si-doped boron carbide: A route to understand amorphization mitigation mechanism. Acta Materialia, 2018, 157, 106-113.	7.9	42

#	Article	IF	CITATIONS
19	Permeability measurements and modeling of topology-optimized metallic 3-D woven lattices. Acta Materialia, 2014, 81, 326-336.	7.9	40
20	Effect of strain rate and dislocation density on the twinning behavior in tantalum. AIP Advances, 2016, 6, .	1.3	40
21	Effect of Alumina on the Structure and Mechanical Properties of Spark Plasma Sintered Boron Carbide. Journal of the American Ceramic Society, 2014, 97, 3710-3718.	3.8	36
22	Microstructural Characterization of a Commercial Hotâ€Pressed Boron Carbide Armor Plate. Journal of the American Ceramic Society, 2016, 99, 2834-2841.	3.8	36
23	Experimental investigation of 3D woven Cu lattices for heat exchanger applications. International Journal of Heat and Mass Transfer, 2016, 96, 296-311.	4.8	34
24	Breaking the icosahedra in boron carbide. Proceedings of the National Academy of Sciences of the United States of America, 2016, 113, 12012-12016.	7.1	31
25	The effect of Si on the microstructure and mechanical properties of spark plasma sintered boron carbide. Materials Characterization, 2017, 134, 274-278.	4.4	31
26	Development of Ni-based superalloys for microelectromechanical systems. Scripta Materialia, 2012, 67, 459-462.	5.2	28
27	Emerging materials for microelectromechanical systems at elevated temperatures. Journal of Materials Research, 2014, 29, 1597-1608.	2.6	26
28	Tailoring the mechanical properties of sputter deposited nanotwinned nickel-molybdenum-tungsten films. Acta Materialia, 2018, 144, 216-225.	7.9	26
29	Tuning the deformation mechanisms of boron carbide via silicon doping. Science Advances, 2019, 5, eaay0352.	10.3	26
30	Experimental quantification of mechanically induced boundary migration in nanocrystalline copper films. Acta Materialia, 2017, 140, 46-55.	7.9	24
31	Nanoscale elastic strain mapping of polycrystalline materials. Materials Research Letters, 2018, 6, 249-254.	8.7	24
32	In Situ Measurement of the Toughness of the Interface Between a Thermal Barrier Coating and a Ni Alloy. Journal of the American Ceramic Society, 2011, 94, s120.	3.8	22
33	Observations of nanocrystalline cubic boron nitride formed with plasma spraying. Acta Materialia, 2016, 116, 155-165.	7.9	20
34	Damping behavior of 3D woven metallic lattice materials. Scripta Materialia, 2015, 106, 1-4.	5.2	19
35	Fabrication and characterization of arc melted Si/B co-doped boron carbide. Journal of the European Ceramic Society, 2019, 39, 5156-5166.	5.7	17
36	Fabrication of dense B4C-preceramic polymer derived SiC composite. Journal of the European Ceramic Society, 2019, 39, 718-725.	5.7	17

#	Article	IF	CITATIONS
37	Development of a High-Temperature Tensile Tester for Micromechanical Characterization of Materials Supporting Meso-Scale ICME Models. Jom, 2016, 68, 2754-2760.	1.9	16
38	Formation of BN from BCNO and the development of ordered BN structure: I. Synthesis of BCNO with various chemistries and degrees of crystallinity and reaction mechanism on BN formation. Ceramics International, 2018, 44, 14980-14989.	4.8	16
39	Topology Optimization of Three-Dimensional Woven Materials Using a Ground Structure Design Variable Representation. Journal of Mechanical Design, Transactions of the ASME, 2019, 141, .	2.9	15
40	On anomalous strain hardening in iridium crystals. Scripta Materialia, 2007, 56, 389-392.	5.2	14
41	Properties of sputter deposited Ni-base superalloys for microelectromechanical systems. Thin Solid Films, 2014, 558, 20-23.	1.8	14
42	Nanotwin formation in Ni–Mo–W alloys deposited by dc magnetron sputtering. Scripta Materialia, 2020, 186, 247-252.	5.2	14
43	Experimental observations of the mechanisms associated with the high hardening and low strain to failure of magnesium. Materialia, 2019, 8, 100504.	2.7	13
44	Investigating the compressive strength and strain localization of nanotwinned nickel alloys. Acta Materialia, 2021, 204, 116507.	7.9	13
45	Precipitation of AlN in a commercial hot-pressed boron carbide. Scripta Materialia, 2015, 101, 95-98.	5.2	12
46	An etÂal. Reply:. Physical Review Letters, 2017, 118, 089602.	7.8	12
47	Experimental observations of twin formation during thermal annealing of nanocrystalline copper films using orientation mapping. Scripta Materialia, 2017, 141, 76-79.	5.2	12
48	Small amount TiB ₂ addition into B ₄ C through sputter deposition and hot pressing. Journal of the American Ceramic Society, 2019, 102, 4421-4426.	3.8	12
49	Twin boundary migration mechanisms in quasi-statically compressed and plate-impacted Mg single crystals. Science Advances, 2021, 7, eabg3443.	10.3	12
50	The mechanical response of additively manufactured IN625 thin-walled structures. Scripta Materialia, 2021, 205, 114188.	5.2	11
51	Addressing amorphization and transgranular fracture of B ₄ C through Si doping and TiB ₂ microparticle reinforcing. Journal of the American Ceramic Society, 2022, 105, 2959-2977.	3.8	11
52	Observations of explosion phase boron nitride formed by emulsion detonation synthesis. Scripta Materialia, 2018, 145, 126-130.	5.2	10
53	Granular flow of an advanced ceramic under ultra-high strain rates and high pressures. Journal of the Mechanics and Physics of Solids, 2020, 143, 104031.	4.8	10
54	Tailoring the coefficient of thermal expansion of ternary nickel alloys through compositional control and non-contact measurements. Journal of Alloys and Compounds, 2020, 833, 155024.	5.5	10

#	Article	IF	CITATIONS
55	Formation of metastable wurtzite phase boron nitride by emulsion detonation synthesis. Journal of the American Ceramic Society, 2018, 101, 3276-3281.	3.8	9
56	Influence of a nanotwinned, nanocrystalline microstructure on aging of a Ni-25Mo-8Cr superalloy. Acta Materialia, 2018, 156, 411-419.	7.9	9
57	Dynamic failure mechanisms of granular boron carbide under multi-axial high-strain-rate loading. Scripta Materialia, 2019, 173, 125-128.	5.2	9
58	Automated methods for the quantification of 3D woven architectures. Materials Characterization, 2017, 124, 241-249.	4.4	8
59	Non-dissociated <c+a> dislocations in an AZ31 alloy revealed by transmission electron microscopy. Materials Research Letters, 2020, 8, 145-150.</c+a>	8.7	8
60	Growth of high purity zone-refined Boron Carbide single crystals by Laser Diode Floating Zone method. Journal of Crystal Growth, 2020, 543, 125700.	1.5	8
61	Mechanical characterization of boron carbide single crystals. Journal of the American Ceramic Society, 2022, 105, 3030-3042.	3.8	8
62	Strong Impact of Minor Elements on the Microstructural Evolution of an Additively Manufactured Inconel 625 Alloy. Metallurgical and Materials Transactions A: Physical Metallurgy and Materials Science, 2022, 53, 2926-2942.	2.2	8
63	Nano-scale Elastic Strain Maps of Twins in Magnesium Alloys. Microscopy and Microanalysis, 2018, 24, 970-971.	0.4	7
64	Bending Nanoindentation and Plasticity Noise in FCC Single and Polycrystals. Crystals, 2019, 9, 652.	2.2	7
65	Small-scale mechanical characterization of space-exposed fluorinated ethylene propylene recovered from the Hubble Space Telescope. Polymer Testing, 2013, 32, 602-607.	4.8	6
66	Effect of synthesis conditions of BCNO on the formation and structural ordering of BN at 1200â€Â°C and 1†GPa. Diamond and Related Materials, 2018, 87, 156-162.	3.9	6
67	Effect of stress-relief heat treatments on the microstructure and mechanical response of additively manufactured IN625 thin-walled elements. Materials Science & Engineering A: Structural Materials: Properties, Microstructure and Processing, 2022, 846, 143288.	5.6	6
68	Fabrication of Freestanding Metallic Ni-Mo-W Microcantilever Beams With High Dimensional Stability. Journal of Microelectromechanical Systems, 2020, 29, 329-337.	2.5	5
69	Intrinsic strengthening and toughening in hexagonal boron nitride by ripples. Acta Materialia, 2022, 229, 117845.	7.9	5
70	Effect of Boron on Microstructure and Fracture of Sintered Ultrafine-Grained Tungsten. Jom, 2018, 70, 2537-2543.	1.9	4
71	Experimental observations of amorphization in multiple generations of boron carbide. Journal of the American Ceramic Society, 2022, 105, 3008-3029.	3.8	4
72	Mechanical Properties of Al Thin Films as Measured by Bulge Testing. Materials Research Society Symposia Proceedings, 1999, 594, 135.	0.1	3

#	Article	IF	CITATIONS
73	The mechanical behavior of single crystal and polycrystalline pure magnesium. Mechanics of Materials, 2021, 163, 104078.	3.2	2
74	Characterization and understanding of the tilt-dependence of core-loss spectra for hexagonal boron nitride. Scripta Materialia, 2021, 204, 114160.	5.2	2
75	In Situ Analysis of the Fracture Behavior of Nanocrystalline Copper Using Precession-Assisted Crystal Orientation Mapping. Microscopy and Microanalysis, 2015, 21, 273-274.	0.4	1
76	Revealing the Microstructural Information of the Quasi-Plastic Zone in a Boron Carbide Using the Advanced Precession Electron Diffraction Technique. Microscopy and Microanalysis, 2019, 25, 788-789.	0.4	1
77	TMS: Advocating for the importance of science and technology. Jom, 2009, 61, 16-16.	1.9	0
78	Manufacturing and Fracture Behavior of Large Scale Multilayered Metal-Ceramic Nanocomposites. Materials Research Society Symposia Proceedings, 2014, 1650, 1.	0.1	0
79	On the formation of arrays of micro-tunnels in pyrope and almandine garnets. American Mineralogist, 2021, 106, 1026-1029.	1.9	0